Journal of Electrical Engineering & Technology (2022) 17:475–484
https://doi.org/10.1007/s42835-021-00817-2

ORIGINAL ARTICLE

A Comparative Study on the Insulation Ageing of 10 kV XLPE Cable via Accelerated Electrical Test and Accelerated Water Tree Test

Weiwei Li[1] · Wenyue Zheng[2] · Lulu Ren[2] · Huan Li[3] · Xuetong Zhao[2] · Can Wang[2] · Jianying Li[4]

Received: 3 December 2020 / Revised: 8 March 2021 / Accepted: 2 June 2021 / Published online: 8 June 2021

Abstract
Medium and high voltage XLPE cables were widely used in urban distribution network. The electric-thermal effect of the cable conductor and water in the running environment are two important factors that cause ageing of cable insulating material. In this work, accelerated electrical test (AET) and accelerated water tree test (AWTT) on 10 kV XLPE cable were carried out for 1440 h, 2880 h and 4320 h, respectively. The physicochemical and dielectric properties of both aged and unaged XLPE samples were tested. Physicochemical investigation of Fourier Transform Infrared (FTIR) spectroscopy and X-Ray Diffraction (XRD) show that higher carbonyl groups index, and lower crystallinity of the XLPE insulating materials were generated in AWTT process than that in AET process. The thermal decomposition process of the AWTT XLPE are complicated, presenting a multi-peak phenomenon in the differential thermogravimetry (DTG) curve. The insulating strength of the samples after AWTT is monotonically decreased from 23.03 kV to 21.74 kV with ageing time. The dielectric properties show that the permittivity and dielectric loss of AWTT samples increased more severely than that of AET samples, with a new dielectric relaxation peak appearing at around 100 Hz. The combination of physicochemical and dielectric results reveals that AWTT process leads to more serious degradation for XLPE insulating materials. A schematic illustration is given to elucidate the development of micro defects in XLPE during the AET and AWTT processes.

Keywords Accelerated electrical test · Accelerated water tree test · Dielectric property · Physicochemical property · XLPE cable

1 Introduction

The great demands for crosslinked polyethylene (XLPE) in the worldwide market is ascribed to its excellent electrical insulating properties, outstanding physicochemical characteristics, easy processing and low cost. Nowadays, the medium and high voltage power cables with the XLPE insulation have been widely used in underground transmission and distribution power system [1–3]. However, degradation of XLPE insulation is still one of the most important problems that causes cable failure during its service life.

Under normal service conditions, the operating temperature of cable insulation is around 90 °C due to the large ampacity. Sometimes the maximum temperature up to 150 °C caused by short circuit or overload is allowed in a short term [4, 5]. Therefore, electric-thermal ageing becomes a main origin of irreversible damage of the cable insulation. For most polymer materials, degradation process is often dominated by oxidation reaction when running or ageing in an oxidizing atmosphere [6]. Afterwards, chain scission and carbonyl groups are produced [7]. The impact of oxidation reaction on XLPE insulation has been studied for decades. It is reported that the lamellas and spherulites could be destroyed, and free volume could be formed in XLPE insulation, resulting in a reduced crystallinity and

✉ Xuetong Zhao
zxt201314@cqu.edu.cn

1 State Grid Sichuan Electric Power Research Institute, Chengdu, Sichuan 610072, People's Republic of China

2 State Key Laboratory of Power Transmission Equipment & System Security and New Technology, Chongqing University, Shapingba District, Chongqing 400044, People's Republic of China

3 School of Electrical Engineering, Shaanxi University of Technology, Hanzhong 723001, People's Republic of China

4 State Key Laboratory of Electrical Insulation and Power Equipment, Xi'an Jiaotong University, Xi'an 710049, People's Republic of China

degraded electrical and mechanical characteristics [8, 9]. Some additives, e.g., dicumyl peroxide (DCP) and phenolic or sulfur-type antioxidants, have been used to mitigate the electric-thermal ageing of XLPE [10, 11]. Actually, antioxidants can play a role in restraining the acceleration of oxidation process, but it can't totally prevent it. In the service of power cables, the effect of electrical filed applied on the XLPE insulation can not be neglected. He D. et al. reported electrical-thermal degradation of 10 kV XLPE insulation aged under an AC voltage of 26.1 kV and 103–135 °C for 150–375 days [12]. The mechanical strength and electrical breakdown field of the XLPE samples were decreased sharply with ageing time when the applied temperature is at 135 °C. Montanari et al. investigated the electrical behavior of the cable models with a thin insulation layer under a long-term electrical-thermal aging, which can give some guidance in the cable design [13]. Wang X. et al. studied the space charge characteristics of XPLE films modified with nanoparticles under a DC voltage of 40 kV and 60 °C for 30–90 days [14].

Electrical-thermal ageing is the main factor causing insulation degradation when the XLPE cables serve in a dry environment. However, water can be introduced into the XLPE insulation during manufacture, storage and installation. In the practical service condition, water might also enter into insulation from the joints or terminals, inducing growth of water tree in the XLPE insulation. Water tree is a common ageing phenomenon that can impair XLPE insulation, which can convert into electrical tree subsequently, increasing failure rate of cables. It becomes another important cause for insulation failure of in-service XLPE power cables. Furthermore, some microscopic defects such as impurities, micro cracks, and scratches in cable insulation might be generated during the manufacturing, transportation, constructing and operating processes [15]. These defects tend to become the starting point for the growth of water trees for cables served in a moist environment. Many measures such as water barriers, semicon cleanliness, and laying practices were adopted to make cables more resistant to water treeing [16]. XLPE cable with water tree retardant additives (often referred to simply as TR-XLPE) is now widespread [17]. However, even though great achievements have been acquired on cable quality in recent years, the power cable running underground is still vulnerable to water tree degradation.

Electric-thermal ageing and water tree degradation are two significant issues endangering the normal operation of XLPE cables. Therefore, accelerated electrical test (AET) and accelerated water tree tests (AWTT), as two important ways to study the degradation processes of XLPE were widely reported [6, 8, 17–19]. However, they have been studied separately, not highlighting the discrepancy caused by water. There is still a lack of comparative investigation on the accelerated electrical test and accelerated water tree tests for XLPE cable. In this work, AET and AWTT are conducted on 10 kV XLPE cables. The differences in physicochemical and dielectric properties caused by those two ageing processes are displayed.

2 Samples and Experiments

2.1 Sample Preparation

Based on the recommendations of standard AEIC CS8-07 and ICEA S-97–682, AET and AWTT on 10 kV XLPE cables were carried out. The ageing conditions of the XLPE samples are shown in Table 1.

For the accelerated electrical test, the cables are put in ambient air and heated by inductive current generated in the conductor loop. The cables were heated up by a straight-through transformer (BCX-15KVA) and kept at between 95 and 100 °C for 8 h and then cooled down to room temperature for 16 h to imitate a load circle every day. During the ageing process, a power frequency voltage of 27.5 kV (TNS(SVC)100KVA) is applied. During the AWTT process, the cables were put in tubes filled with tap water, and the schematic and object diagrams were shown in Fig. 1a and b. The ageing test was divided into three stages at regular intervals for 1440 h (phase 1), 2880 h (phase 2) and 4320 h (phase 3), and the samples were denoted as AET-1440 h, AET-2880 h, AET-4320 h for accelerated electrical ageing, and AWTT-1440 h, AWTT-2880 h, AWTT-4320 h for accelerated water-tree ageing. Three cables are selected to experimental test under each condition in this work.

2.2 Physicochemical and Electrical Experiments

For the physicochemical and dielectric properties test, the XLPE slices were cut from the cable insulation layer by using J/Q XLPE cable slicer. FTIR spectrometer (model IR Prestige-21) was employed to analyze the variation of XLPE molecular structure in the ageing process. All the samples mentioned above were measured in the range of 500–4000. 1 cm × 1 cm XLPE samples were prepared for X-ray diffraction test, and were scanned with a DX-1000 X-ray diffractometer from 15° to 30° with a scan step rate of 0.026 °. TGA/SDTA851 from Mettler Toledo was used

Table 1 The ageing conditions of XLPE cable samples

Aging model	Environment condition	E (kV)	T (°C)	Heating time (h)	Cooling time (h)
AET	Air	27.5	95–100	8	16
AWTT	Water	27.5	95–100	8	16

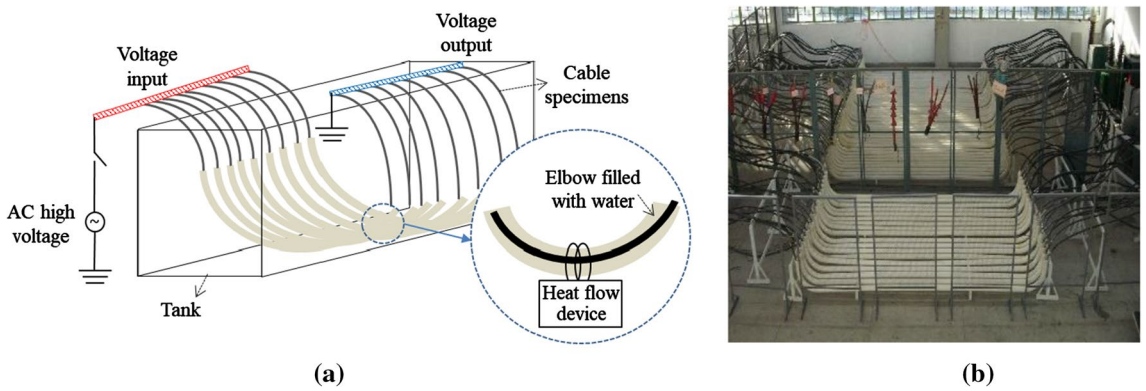

Fig. 1 The AWTT schematic **a** and object **b** diagrams for 10 kV XLPE cable

to analyze the thermal decomposition behavior of XLPE samples. 10–20 mg samples were prepared and put in an alumina crucible, and the test temperature went from room temperature to 600 °C by rate of 20℃/min. During the whole test process, argon gas flow of 50 ml/min was used for protection. 35 mm × 35 mm square samples with thickness of 0.2 mm were cut from the cable insulation layer for the insulating strength test in accordance with the IEC 60243-1-1998 ("Methods of Test for Electric Strength of Insulating Materials"). In the test, 50 Hz AC voltage was applied, and the voltage increasing speed was 500 V/s. At least 10 breakdown points were carried out for each kind of sample. Round-disk XLPE samples with diameter of 10 mm and thickness of 0.5 mm were prepared for the dielectric test, and gold was sputtered onto both sides of the samples as conductive electrodes. The dielectric properties were measured with Novocontrol broadband dielectric spectrometer (Concept 80, Germany) in the frequency range from 1 to 10^5 Hz.

3 Results and Discussion

3.1 FTIR Results

The FTIR spectra of both unaged and aged XLPE samples are shown in Fig. 2a and b. We can see that the absorption peaks at the values between 1700 and 1750 are obviously intensified after AET and AWTT ageing. As well known, carbonyl groups (C = O) is a typical oxidation product in XLPE, which can be an indicator of thermo-oxidative ageing. The absorption peaks of carbonyl groups appear between 1700 and 1800, which mainly contains ester groups (-COO-) at 1760, aldehyde groups (-CHO) at 1738, and keto-groups (-CO-) at 1720, respectively [19]. Carbonyl index (*CI*) was calculated based on the ratio of absorption

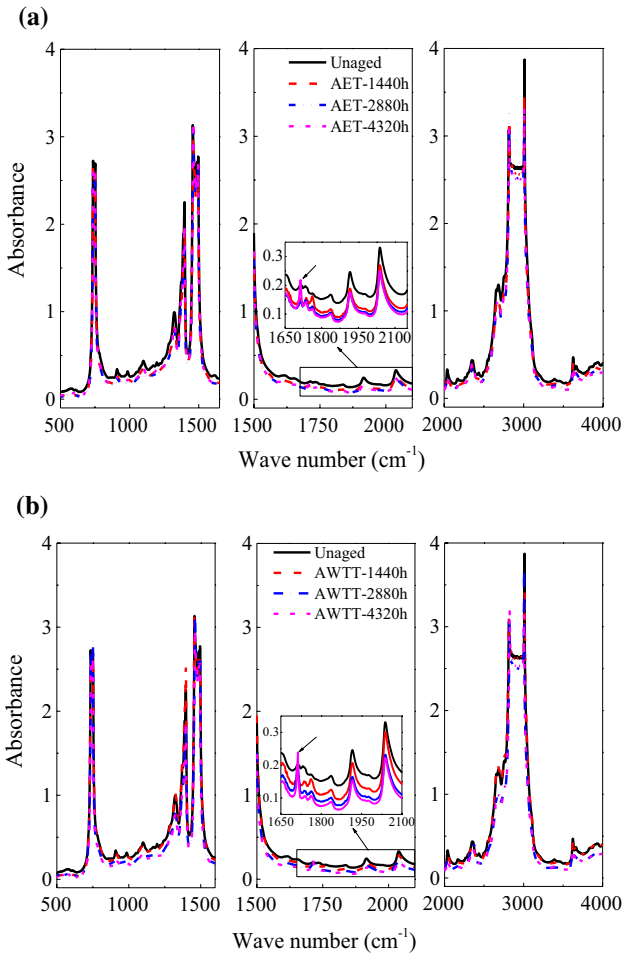

Fig. 2 FTIR Spectra of different XLPE samples. **a** Accelerated electrical test. **b** Accelerated water tree test

peak at 1720 cm^{-1} and 2010 cm^{-1}, which is commonly used to quantify the oxidation degree [12, 20, 21]. The value of *CI* can be calculated as follows:

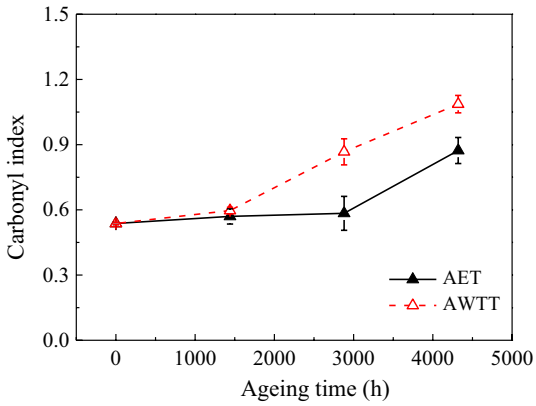

Fig. 3 Variation of the Carbonyl index with the ageing time

$$CI = \frac{I_{1720}}{I_{2010}} \tag{1}$$

where I_{1720} and I_{2010} are the absorption peak intensity of at 1720 cm^{-1} and 2010 cm^{-1}, respectively. As shown in Fig. 3, the carbonyl index is about 0.53 for the unaged XLPE sample, which means there are just a few carbonyl group residuals during the manufacturing process [22]. However, the values of carbonyl index of XLPE increased to 0.87 and 1.10 for the AET-4320 h and AWTT-4320 h samples, respectively. AWTT induces a higher carbonyl index, indicating that water or moist environment act as degradation catalysts to accelerate the decomposition process of XLPE.

3.2 XRD Results

The X-ray diffraction (XRD) patterns of both unaged and aged XLPE samples are shown in Fig. 4a and b. A typical XRD curve of the unaged sample shows an amorphous halo at $2\theta = 21.1°$ (peak 1) and two major crystalline peaks at $2\theta = 21.7°$ (peak 2) and $2\theta = 24.1°$ (peak 3), corresponding to the (110) and the (200) lattice planes [22, 23]. Another tiny peak (peak 4) appeared at around $2\theta = 26.8°$ is related to the plane lattice of (020) as Miller indexes [22]. The results present that the XRD curves do not show any new crystalline peaks or obvious changes in the position of crystalline peaks. It indicates that AET and AWTT process do not induce any new crystalline phases in the materials structure, but the major crystalline peak at 21.7°is greatly decreased after AET and AWTT ageing.

As shown in Fig. 4c, the crystallinity of XLPE samples were calculated using Hinrichsen's method [24] that is based on fitting the XRD spectra into three different Gaussian functions by ORIGIN 9.0 software with the following relationship:

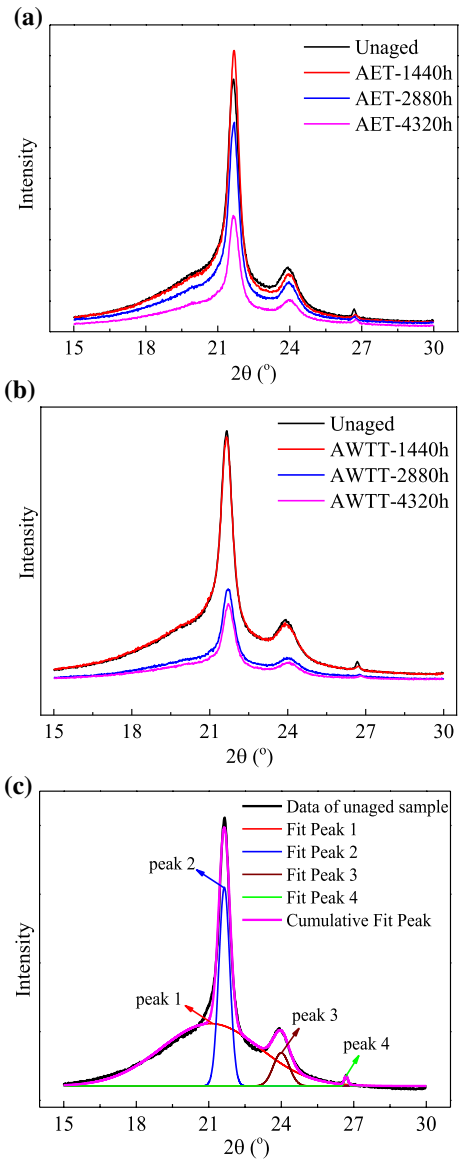

Fig. 4 X-ray diffraction patterns of **a** AET XLPE samples, **b** AWTT XLPE samples, **c** the Gaussian Fitting for the XRD spectra of the amorphous regions and the crystalline regions of the typical unaged XLPE sample

$$x(\%) = \frac{area2 + area3 + area4}{area1 + area2 + area3 + area4} \times 100\% \tag{2}$$

where $\chi(\%)$ is the crystallinity percentage, area 1 corresponds to the amorphous halo, areas 2, area 3 and area 4 correspond to the crystalline peaks at 21.7° (peak 2), 24.1° (peak 3) and 26.8° (peak 4), respectively.

Figure 5 presents the variations of crystallinity with the ageing time. For the AET sample, the crystallinity increases a little firstly when the ageing time reaches around 1500 h, and then goes down. Li et al. found the similar phenomenon in the thermo-oxidative aged XLPE, and the increase

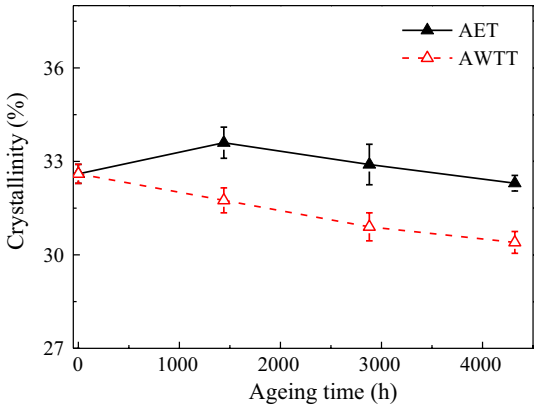

Fig. 5 The crystallinity of XLPE samples with the different AET and AWTT

of crystallinity in the initial ageing stage is attributed to recrystallization of XLPE with favors of the alignment of the chains that were imperfectly crystallized in the manufacturing process [22]. However, the crystallinity of AWTT samples is reduced during the whole ageing time.

3.3 Thermogravimetric Analysis

Figure 6 displays typical thermogravimetric analysis (TGA) and derivative thermogravimetric (DTG) curves of AET and AWTT XLPE samples. It is find that the decomposition process starts at the temperature of 450 °C and ended at the temperature around 500 oC. In the inset of Fig. 6a, the DTG curve of the AET sample presents a peak that corresponds to the fastest decomposition temperature $T_{d\text{-}1}$. The peak shifts to lower temperature, i.e. from 492 to 488 °C with the increases of ageing time, which demonstrated that the thermal stability of the samples was deteriorated with the increase of the ageing time. Activation energies for the XLPE decomposition were determined using the Coast-Redfern approach [25], which shows that the activation energy increases a little from 3.44 to 3.48 eV in the first stage of AET sample (before 1440 h) and then decreases to 3.37 eV with the further ageing period, as listed in Table 2. In accordance with the XRD result, the crystallinity increases due to recrystallization of XLPE, which may make crosslinked XLPE molecules difficult to decompose in the initial ageing stage. However, the DTG curves of AWTT samples present an abnormal multi-peak phenomenon and several fastest decomposition temperature $T_{d\text{-}1}$, $T_{d\text{-}2}$, and $T_{d\text{-}3}$ can be obtained, indicating that there exist different main stages during the thermal decomposition process. The activation energies corresponding to $T_{d\text{-}1}$, $T_{d\text{-}2}$, and $T_{d\text{-}3}$ were calculated based on the Coast-Redfern approach and presented in the Table 2. Taking the sample of AWTT-4320 h for example, the activation energies of the three decomposition processes

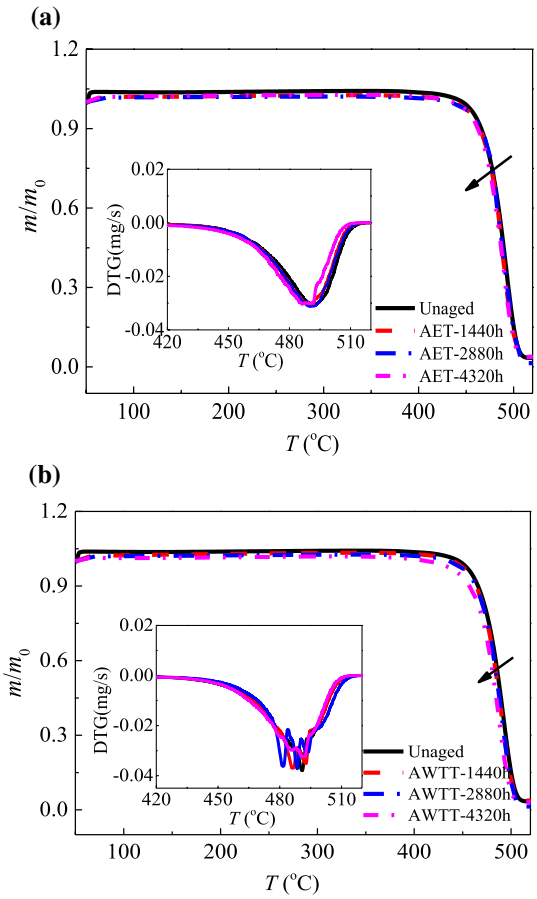

Fig. 6 The TGA and DTG curves of XLPE samples with the different **a** AET and **b** AWTT

($T_{d\text{-}1}$, $T_{d\text{-}2}$, and $T_{d\text{-}3}$) were 3.38, 3.16 and 3.04 eV, respectively. The activation energies of the decomposition related to $T_{d\text{-}2}$, and $T_{d\text{-}3}$ is much lower.

As shown in Fig. 5, the crystallinity of AWTT samples decreases with the ageing time. Therefore, it is believed that a mass of microscopic defects may be generated because some crystalline region (lamellae) in XLPE can be broken under the multiple effects of electric, thermal oxidation reaction, and water. Especially, the dielectrophoresis force caused by water molecules can significantly promote degradation of XLPE molecular chains [26]. Furthermore, some low-density areas can be formed in the cable insulation which may be more easily decomposed and thus resulted in the multi-peak phenomenon in the DTG curves.

3.4 Insulating Strength

Figure 7 shows the Weibull plots of insulating strength under power frequency voltage. The results in Table 3 present the calculated Weibull scale and shape parameters (α and β). α is the breakdown voltage in the confidence interval of 63.2%

Table 2 Parameters obtained from TGA and DTG measurement

Samples	$T_{d\text{-}1}$ (°C)	$E_{d\text{-}1}$ (eV)	$T_{d\text{-}2}$ (°C)	$E_{d\text{-}2}$ (eV)	$T_{d\text{-}3}$ (°C)	$E_{d\text{-}3}$ (eV)
Unaged	492	3.44	/	/	/	/
AET-1440 h	491	3.48	/	/	/	/
AET-2880 h	490	3.38	/	/	/	/
AET-4320 h	488	3.37	/	/	/	/
AWTT-1440 h	492	3.41	486	3.27	/	/
AWTT-2880 h	491	3.39	488	3.25	481	3.13
AWTT-4320 h	490	3.38	485	3.16	479	3.04

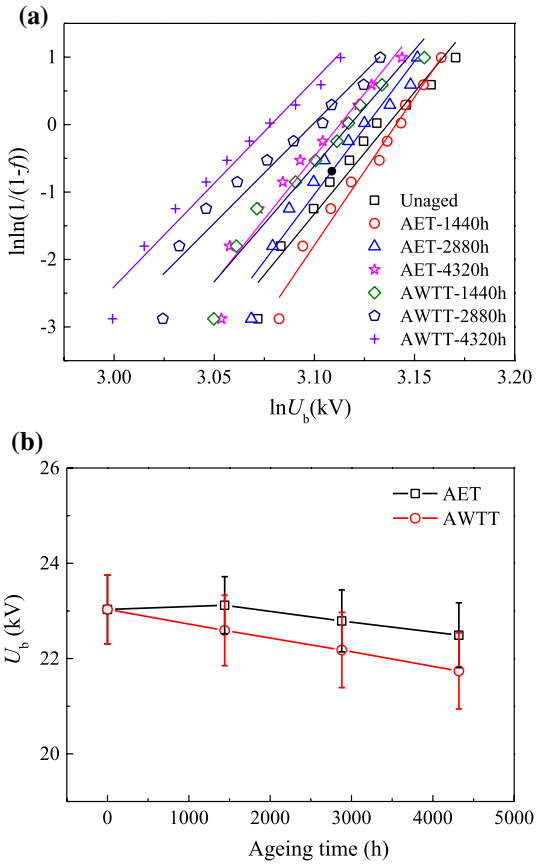

Fig. 7 **a** Weibull plots and **b** insulating strength of AET and AWTT samples

and β displays the data scatter. A higher β represents a narrower range in breakdown voltage. For the AET samples, the breakdown voltage shows an initially increase a little, and then decrease from 23.03 kV to 22.49 kV with ageing time. It has a similar evolution trend with that of the crystallinity of XLPE. The similar phenomenon was reported in other reports [12, 19], which indicates that the insulating strength of XLPE may be closely related with the crystalline morphology. However, for the AWTT samples, the breakdown voltage is monotonically decreases from 23.03 kV to 21.74 kV with ageing time the for AWTT samples. The insulating strength of the samples were not reduced greatly after the AET and AWTT in this work.

Table 3 The parameters of Weibull distribution under power frequency voltage

Samples	Shape parameter (β)	Scale parameter (α/kV)
Unaged	36.1	23.03
AET-1440 h	43.9	23.12
AET-2880 h	39.49	22.79
AET-4320 h	37.2	22.49
AWTT-1440 h	34.34	22.59
AWTT-2880 h	29.78	22.18
AWTT-4320 h	30.64	21.74

3.5 Dielectric Results

Figure 8 depicts the frequency dependence of real and imaginary parts of permittivity (ε', ε'') for the aged and unaged XLPE samples. As presented in Fig. 8a, the ε' of unaged sample is ~ 2.5, however, the value is enhanced to 2.9 and 3.25 for the AET and AWTT samples (AET-4320 h and AWTT-4320 h), respectively. In Fig. 8b, the ε'' of AET samples was significantly increased at low frequency (< 50 Hz), which can be attributed to the contribution of enhanced dc conductivity according to the Debye Eq. (3).

$$\varepsilon^*(\omega) = \varepsilon'(\omega) - j\varepsilon''(\omega) = \varepsilon_\infty + \frac{\varepsilon_s - \varepsilon_\infty}{1+\omega^2\tau^2} - j\left(\frac{\sigma_0}{\omega\varepsilon_0} + \frac{(\varepsilon_s - \varepsilon_\infty)\omega\tau}{1+\omega^2\tau^2}\right) \quad (3)$$

where ε_s and ε_∞ denote the static and optical permittivity, respectively, ω is the angular frequency, τ is the dipolar relaxation time, σ_0 is the direct current (dc) conductivity.

For the AWTT sample, the ε' shows an apparent decline trend with applied frequency from 1 to 100 Hz, and an obvious relaxation peak can be found at around 100 Hz, which was reported and considered as the interfacial polarization due molecular chains segments or microdefect caused by AWTT process [18, 27–29]. Below 10 Hz,

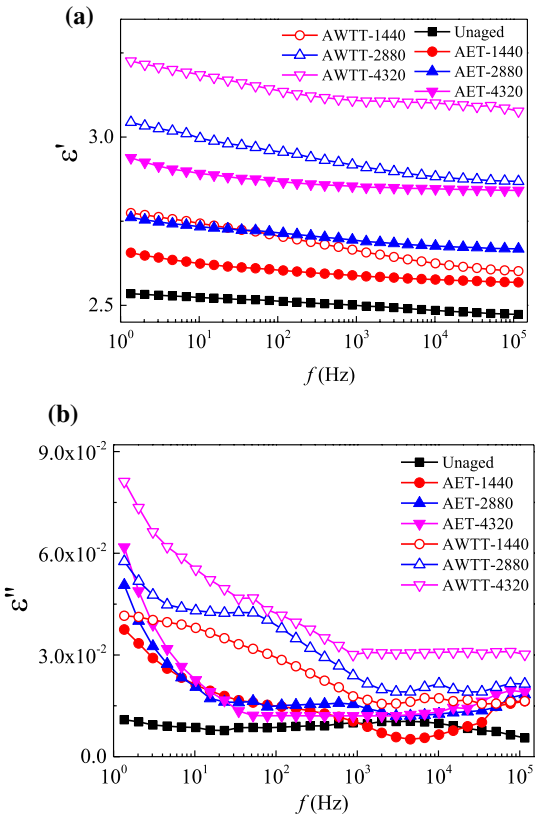

Fig. 8 Temperature dependences of ε' **a** and ε'' **b** of XLPE samples with the different AET and AWTT

the dielectric loss was dominated by dc conductivity. In addition, at the same ageing stage, the permittivity and dielectric loss of the AWTT samples is obviously higher than that of the AET samples in the whole applied frequency. It indicates that AWTT process can induce a more serious degradation in the dielectric properties of XLEP insulation due to the incorporation of moisture ingress and water tree [30].

3.6 The Micro-Level Analysis of Defects

It is known that the microstructure of XLPE insulation generally consists of spherulites (crystalline lamellar ribbons) and amorphous phase as shown in Fig. 9a. The interface between the crystalline and amorphous area is generally regarded as weak point, where the microdefects such as voids in XLPE may easily formed and developed during the AET or AWTT ageing processes. In the amorphous region between lamellar ribbons, the molecular chains are linked via inter-molecular Van der Waals bonds, which is vulnerable to the continuous electric-thermal ageing as well as oxidation reaction [31–33], leading to free volume rearrangement and formation of submicrocavities. In Fig. 9b, two adjacent lamellas from spherulite are selected to illustrate the change of crystalline structure of XLPE insulation during the AET ageing process. Thermal swelling force (σ_1) is applied on the vertical direction of lamellas due to thermal expansion of amorphous inter-lamellar phase, leading to a growing lamella space. Thus oxygen can diffuse into spherulite more easily, promoting oxidizing reaction and breaking the molecular chains that connects lamellas. Moreover, under the applied electrical filed, space charge such as electrons and charged particles can be accumulated in the interface between the crystalline and amorphous area or in the submicrocavities of the XLPE insulation, which may cause seriously electric field distortion and energy transfer in the XLPE insulation [12, 34]. Electrons can be accelerated under the distorted electrical filed and break molecular chains. After a long-term AET process, the folded chains between lamellas can be broken, and the lamella structure may be destroyed, resulting in a low crystallinity of XLPE.

As shown in Fig. 9c, water may immerse into the cable insulating materials in AWTT process so that another dielectrophoresis force σ_2 may be introduced. With the increase of ageing time, water molecules will permeate into amorphous region in depth and enlarge the angle between two lamellar

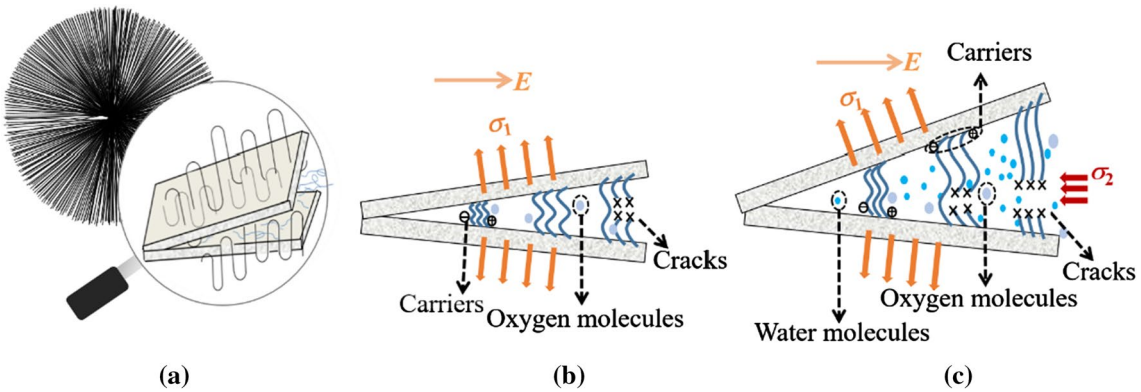

Fig. 9 **a** The microstructure of spherulites and lamellas, the development of XLPE degradation during **b** AET and **c** AWTT ageing processes

ribbons [35, 36], thus cause more severe degradation of XLPE insulation. Since tap water was used in the AWTT process, some impurities like metal ions and carboxylates may work as carriers in the interface between amorphous and lamellar zones, which was noticed and reported by several researchers in the research of water tree [37, 38] and electrical tree [36, 39]. It was found by TEM observation that the initial electrical tree grew along the lamellar layer [36, 39]. These results support that lamellar/amorphous interface in the insulation layer may work as channels of water during AWTT ageing and consequently lead to the change of physical, chemical and electrical performance. L.A. Dissado et al. [40] proposed that extended states of carriers can lie in between the chains in the crystals or in the region of unfulfilled lattice sites in the amorphous region. Moreover, interfacial polarization caused by the carriers can happen in the interface between crystalline and amorphous area or the submicrocavities, and results in a high dielectric loss in low frequency range [41]. The impurity introduced with water can also enhance the electric conduction and lead to thermionic polarization process [42]. As a consequence, AWTT process gave rise to a more severe degradation in the XLPE insulating materials.

4 Conclusion

This work studied the effect of accelerated electrical test and accelerated water tree test on the physicochemical and dielectric properties of 10 kV XLPE cable. The AWTT combines the functions of water and electricity, inducing higher carbonyl index, lower decomposition activation energy and lower crystallinity than AET process. During AWTT process, oxygen-containing groups which have various decomposition temperatures may cause the multi-peak phenomenon in DTG curve. The dielectric loss of AWTT samples is higher than that of AET samples, and a new dielectric relaxation can be observed due to polarization relaxation at around 100 Hz. All in all, AWTT process can lead to a more severe degradation due to superimposition of moisture and electrical stress. A schematic diagram is proposed to illustrate the microstructure evolution of XLPE insulation during AET and AWTT process. Thermal swelling force and dielectrophoresis force are two significant factors to break up molecular chains and the spherulites.

Acknowledgements This work was financially supported by the Fund of the National Natural Science Foundation of China (No. 51877016), the Natural Science Foundation of Chongqing (No. cstc2019jcyj-xfkxX0008), and the Fok Ying-Tong Education Foundation, China (No. 171050).

Author's Contribution WL Investigation, Data curation. WZ Writing—original draft. LR Software, Data curation. HL Data collection and curation. XZ Investigation, Writing—review & editing Funding acquisition, CW Visualization. JL Conceptualization, Supervision.

Declarations

Conflict of interest The authors declare that they have no conflict of interest.

References

1. Nikolajevic SV (1993) Investigation of water effects on degradation of crosslinked polyethylene (XLPE) insulation. IEEE Trans Power Delivery 8(4):1682–1688
2. Gulmine JV, Akcelrud L (2006) Correlations between structure and accelerated artificial ageing of XLPE. Eur Polym J 42(3):553–562
3. Li JY, Li H, Wang QM, Zhang X, Ouyang BH, Zhao JK (2016) Accelerated inhomogeneous degradation of XLPE insulation caused by copper-rich impurities at elevated temperature. IEEE Trans Dielectr Electr Insul 23(3):1789–1797
4. Anandakumara K, Stonkus DJ (1992) Assessment of oxidative thermal degradation of crosslinked polyethylene and ethylene propylene rubber cable insulation. Polym Eng Sci 32(18):1386–1393
5. Bernstein BS (1989) Service life of crosslinked polyethylene as high voltage cable insulation. Polym Eng Sci 29(2):13–18
6. Nedjar M (2009) Effect of thermal aging on the electrical properties of crosslinked polyethylene. J Appl Polym Sci 111(4):1985–1990
7. Gillen KT, Bernstein R, Clough RL, Celina M (2006) Lifetime predictions for semi-crystalline cable insulation materials: I. Mechanical properties and oxygen consumption measurements on EPR materials. Polym Degrad Stab 91(9):2146–2156
8. Boukezzi L, Nedjar M, Mokhnache L, Lallouani M, Boubakeur A, Ann C (2006) Thermal aging of cross-linked polyethylene. Sci Mat 31(5):561–569
9. Kim C, Jin Z, Jiang P, Zhu Z, Wang G (2006) Investigation of dielectric behavior of thermally aged XLPE cable in the high-frequency range. Polym Test 25(4):553–561
10. Zhao XT, Liao RJ, Liang NC, Yang LJ, Li J, Li JY (2014) Role of defects in determining the electrical properties of ZnO ceramics. J Appl Phys 116(1):014103
11. Sekii Y (2007) Influence of antioxidants and cross-linking on the crystallinity of XLPE dielectrics. 2007 IEEE Conference on electrical insulation and dielectric phenomena, Vancouver, Canada, 14–17
12. He D, Zhang T, Ma M, Gong W, Wang W, Li Q (2020) Research on mechanical, physicochemical and electrical properties of XLPE-insulated cables under electrical-thermal aging. J Nanomater 2020:3968737
13. Montanari GC, Pattini G, Simoni L (1987) Long-term behavior of XLPE insulated cable models. IEEE Trans Power Deliver 2(3):596–602
14. Wang X, Liu Q, Zhang X, Wu K, Zhang C, Li W (2016) Study on space charge behavior of XLPE after long-term aging under temperature gradient and DC stress. 2016 International conference on condition monitoring and diagnosis, Xi'an, China, 741–744
15. Zhou K, Zhao W, Tao XT (2013) Toward understanding the relationship between insulation recovery and micro structure in water tree degraded XLPE cables. IEEE Trans Dielectr Electr Insul 20(6):2135–2142
16. Hampton N, Hartlein R, Lennartsson H, Orton H, Ramachandran R (2007) Long-Life XLPE Insulated Power Cable. 7th

International conference on insulated power cable jicable, Versailles, France, 350–356
17. Platbrood G, Hennuy B, Tits Y, Sutton SJ (2009) Water trees in medium voltage XLPE cables: comparison of different polyethylene insulation using short time accelerated ageing tests. 2009 IEEE Conference on Electrical Insulation and Dielectric Phenomena, Virginia Beach, America, 18–21
18. Li JY, Zhao XT, Yin GL, Li ST, Zhao JK, Ouyang BH (2011) The effect of accelerated water tree ageing on the properties of XLPE cable insulation. IEEE Trans Dielectr Electr Insul 18(5):1562–1569
19. Ouyang BH, Li H, Zhang X, Wang SH, Li JY (2017) The role of micro-structure changes on space charge distribution of XLPE during thermo-oxidative ageing. IEEE Trans Dielectr Electr Insul 24(6):3849–3859
20. Zhang Y, Li S, Gao J, Wang S, Wu K, Li J (2020) Ageing Assessment of XLPE Cable Insulation by Residual Antioxidant Content. IEEE Trans Dielectr Electr Insul 27(6):1795–1802
21. Lv H, Lu T, Xiong L, Zheng X, Huang Y, Ying M, Cai J, Li Z (2020) Assessment of thermally aged XLPE insulation material under extreme operating temperatures. Polym Test 88:106569
22. Gulminea JV, Akcelrud L (2006) FTIR characterization of aged XLPE. Polym Test 25(7):932–942
23. Boukezzi L, Boubakeur A, Lallouani M (2007) Annual Report-Conference on Electrical Insulation and Dielectric Phenomena. 2007 IEEE Conference on Electrical Insulation and Dielectric Phenomena, Vancouver, Canada, 14–17
24. Nath R, Perlman MM (1989) Effect of crystallinity on charge storage in polypropylene and polyethylene. IEEE Trans Elect Insul 24(3):409–412
25. Coats AW, Redfern JP (1964) Kinetic parameters from thermogravimetric data. Nature 201:68–69
26. Tanaka T, Fukuda T, Suzuki S (1976) Water tree formation and lifetime estimation in 3.3 kV and 6.6 kV XLPE and PE power cables. IEEE Trans Power App Syst 47(8):16–21
27. Suraci SV, Fabiani D, Xu A, Roland S, Colin X (2020) Ageing assessment of XLPE LV cables for nuclear applications through physico-chemical and electrical measurements. IEEE Access 8:27086–27096
28. Suraci SV, Fabiani D, Li CY (2019) Additive effect on dielectric spectra of crosslinked polyethylene (XLPE) used in nuclear power plants, In Proceedings of the 2019 IEEE 37th Electrical Insulation Conference (EIC), Calgary, Canada, 410–413
29. Tu DM, Wang XS, Liu FD, Yang BT, Liu YN (1993) The trap theory of breakdown in polymer and its verification in polypropylene. Trans China Electrotechnical Soc 3(3):47–50
30. Sarma H, Cometa E, Densley J (2002) Accelerated ageing tests on polymeric cables using water-filled tanks - a critical review. IEEE Electr Insul Mag 18(2):15–26
31. Parpal JL, Crine JP, Dang C (1997) Electrical aging of extruded dielectric cables. A physical model. IEEE Trans Dielectr Electr Insul 4(2):197–209
32. Li H, Zhai S, Chen J, Hu LB (2019) Review in different size of defect structures in xlpe cable insulation. Insul Mater 52(12):1–9
33. Jones JP, Llewellyn JP, Lewis TJ (2005) The contribution of field-induced morphological change to the electrical aging and breakdown of polyethylene. IEEE Trans Dielectr Electr Insul 12(5):951–966
34. Li WW, Li JY, Wang X, Li ST, Chen G, Zhao JK, Ouyang BH (2014) Physicochemical origin of space charge dynamics for aged XLPE cable insulation. IEEE Trans Elect Insul 21(2):809–820
35. Chen JQ, Zhao H, Xu ZY, Zhang CC, Yang JM, Zheng CJ, Lei JS (2016) Accelerated water tree aging of crosslinked polyethylene with different degrees of crosslinking. Polym Test 56:83–90
36. Hozumi N, Okamoto T, Fukagawa H (1998) TEM observation of electrical tree paths and microstructures in polyethylene. IEEE Int'l Sympos Electr Insul (ISEI), Boston, 331–334
37. Crine JP (1998) Electrical, Chemical and mechanical process in water treeing. IEEE Trans Dielectr Electr Insul 5(5):681–694
38. Raharimalala V, Poggi Y, Filippini JC (1994) Influence of polymer morphology on water treeing. IEEE Trans Dielectr Electr Insul 1(6):1094–1103
39. Okamoto T, Ishida M, Hozumi N (1989) Dielectric breakdown strength affected by the lamellar configuration in XLPE insulation at a semiconducting interface. IEEE Trans Dielectr Electr Insul 24(4):599–607
40. Dissado LA, Fothergill JC (1992) Electrical degradation and breakdown in polymers. Peter peregrinus Ltd, London
41. Ouyang BH, Kang Y, Zhao JK, Zhao XT, Li JY, Li ST (2010) Influence of accelerated water tree aging on insulation of XLPE cables. High Voltage Engineering 36(8):1942–1949
42. Chen JD, Liu ZY (1982) Dielectric physics. China Mechanical Industry Press, Beijing

Weiwei Li was born in Shandong, China, in 1984. She received the B.S and Ph.D. Degrees in electrical engineering from Xi'an Jiaotong University, China, in 2008 and 2013 respectively. She is now a senior engineer in State Grid Sichuan Electric Power Research Institute, China. Her major research interests include high voltage insulation and detecting technology for electrical equipment.

Wenyue Zheng received her bachelor's degree from Northeast Forestry University and is now a postgraduate student at Chongqing University. Her main research field is polymer materials.

Lulu Ren was born in Shanxi, China, in 1994. She received the B.S. Degree in electrical engineering from China University of Petroleum (East China) in 2015. Currently, she is a graduate student at the State Key Laboratory of Power Transmission Equipment & System Security and New Technology in Chongqing University. Her main research field is polymer-based materials for energy storage application and dielectric properties of ceramics.

Huan Li was born in Shaanxi, China, in 1988. He received the Ph.D. degree in electrical engineering from Xi'an Jiaotong University in 2017. Currently, he works in Shaanxi Sci-Tech University. His main research field is failure mechanism of the cable insulation.

Xuetong Zhao was born in Henan, China in 1984. He received the B.S and Ph.D. degree in College of Electrical Engineering from Henan Polytechnic University and Xi'an Jiaotong University, China. Currently, he is now a associate professor at Chongqing University. His main research field is electrical insulation material and varistor ceramics.

Can Wang received her bachelor's degree from Henan Normal University and is now a postgraduate student at Chongqing University. Her main research field is polymer materials.

Jianying Li was born in Shaanxi, China in 1972. He received the B.S, M.S and Ph.D. degrees in electrical engineering from Xi'an Jiaotong University, China in 1993, 1996 and 1999, respectively. He is now a professor at Xi'an Jiaotong University. His major research fields are high voltage insulation and dielectrics.